J. Fluid Mech. (1995), *vol.* 290, *pp.* 213–224

Non-axisymmetric instability of core–annular flow

By HOWARD H. HU AND NEELESH PATANKAR

Department of Mechanical Engineering and Applied Mechanics, University of Pennsylvania, 297 Towne Building, 220 S. 33rd Street, Philadelphia, PA 19104-6315, USA

(Received 13 July 1994 and in revised form 7 December 1994)

Stability of core–annular flow of water and oil in a vertical circular pipe is studied with respect to non-axisymmetric disturbances. Results show that when the oil core is thin, the flow is most unstable to the asymmetric sinuous mode of disturbance, and the core moves in the form of corkscrew waves as observed in experiments. The asymmetric mode of disturbance is the most dangerous mode for quite a wide range of material and flow parameters. This asymmetric mode persists in vertical pipes with upward and downward flows and in horizontal pipes. The analysis also applies to the instability of freely rising axisymmetric cigarette smoke or a thermal plume. The study predicts a unique wavelength for the asymmetric meandering waves.

1. Introduction

There is a strong tendency for two fluids to arrange themselves so that the low-viscosity constituent is in the region of high shear. This gives rise to a kind of gift of nature in which the lubricated flows are stable, and opens up interesting possibilities for technological applications in which one fluid is used to lubricate another. One possible application is lubricated pipelining, the transportation of viscous crude oil with the addition of an immiscible lubricating liquid, usually water. A historical review on this subject was given in the book by Joseph & Renardy (1992).

The hydrodynamic stability of oil and water core–annular flows (CAF) in a horizontal pipe has been studied, for example, by Joseph, Renardy & Renardy (1984), Preziosi, Chen & Joseph (1989), Hu & Joseph (1989). In these studies, the density of two fluids are matched, thus the effect of gravity can be neglected. The most unstable disturbance was found to be axisymmetric under their test conditions. They showed that by correlating the stability profile with experiments, the linear theory of instability could be used as a diagnostic tool in predicting the flow regimes which arise in practice: stable core–annular flow; wavy core flow; bubbles and slugs of oil and water; bubbly mixtures of oil and water; and emulsions, mainly of water in oil. Flow regimes, wavelength and wave speed were predicted with fair accuracy by linear theories. In the limit of small ratio of viscosities of water to oil, Hu, Lundgren & Joseph (1990) and Miesen *et al.* (1992) examined the instability of axisymmetric interfacial waves in core–annular flows.

In the vertical configuration, the effects of the gravity and density difference of two fluids can be easily incorporated into the analysis. Hickox (1971) studied the linear stability of Poiseuille flow of two fluids in a vertical pipe. He limited his attention to long waves and to the case where the fluid viscosity in the core is less than that in the annulus, for example water inside oil, which is of little interest in lubricated pipelining. He found that all such flows are unstable to long waves. Renardy (1987) investigated the instability of a planar three-layer vertical Poiseuille flow of two fluids. Chen, Bai

& Joseph (1990) studied the stability of a vertical core–annular flow in a circular pipe both numerically and experimentally. They verified the prediction of the linear stability theory experimentally for the case of free fall. Under certain flow conditions in their experiments they observed large-amplitude axisymmetric waves (bamboo waves) in the upflow section and corkscrew-shaped waves in the downflow section. In their numerical computation, however, they checked through some parameter space and found that the axisymmetric disturbance was always most unstable, thus restricted their attention to the axisymmetric mode. The same corkscrew-shaped waves were also reported by Freeman & Tavlarides (1979) and Joseph (1990). A more extensive experimental study of the stability of vertical core–annular flow was done by Bai, Chen & Joseph (1992). They documented new flow types that were not achieved in horizontal flows: axisymmetric bamboo waves in upflow and asymmetric corkscrew waves in downflow. They conjectured that the corkscrew waves were analogous to the buckling of a very soft rubber when loaded with shear traction. However, their theory did not predict the occurrence of the corkscrew waves.

Boomkamp & Miesen (1992) examined the stability of non-axisymmetric waves in core–annular flow when the ratio of viscosities of water and oil is small. They found that growth rates of non-axisymmetric and axisymmetric modes are approximately the same, and thus concluded that the non-axisymmetric modes are important and should be taken into account in the description of interfacial waves in core–annular flow.

The instability of a thermal plume in ambient air constitutes a problem similar to core–annular flow. The instability of the plume is characterized by non-axisymmetric deformations. The commonly observed 'meandering' deformation of a rising cigarette smoke illustrates this instability. Lister (1987) analysed the stability of a two-dimensional planar plume of buoyant fluid. He showed that in the limit of long waves the plume is always unstable to varicose disturbances and is also unstable to meandering disturbances if the external fluid viscosity is less than a certain multiple of the internal fluid viscosity. Yang (1992) developed a dispersion equation which accounts for the instability of all transverse modes on a three-dimensional axisymmetric plume. The dispersion equation shows that the dynamic interaction of the ambient air is responsible for the growth of any disturbance on the plume surface, and the sinuous mode has the highest growth rate at all wavenumbers when the density difference between the plume and the surrounding air is small. His theory proved the snake form of the onset of instability of a plume.

In this study, we shall study the stability of core–annular flow in a vertical circular pipe with respect to non-axisymmetric disturbances and compare our theoretical predictions with the recent experiments of Bai *et al.* (1992). We will also examine the stability of freely rising cigarette smoke or a thermal plume.

2. Basic flow

Consider two immiscible fluids flowing inside a vertical pipe in a concentric configuration with the core occupied by fluid 1 and the annulus by fluid 2. The interface between the fluids is located at $r = r_1(\theta, x, t)$, where t is the time and (r, θ, x) are cylindrical coordinates with x in the same direction as the velocity of the core flow. Thus the gravity is acting in the negative x-direction in the upward flow and in the positive x-direction in the downward flow. Let $\boldsymbol{u} = (u_r, u_\theta, u_x)$ be the velocity components and $\hat{p}$ be the pressure. Assume that the pipe is infinitely long with its axis at $r = 0$, and that the mean radius of the interface $r = r_1(\theta, x, t)$ over $\theta (0 \leqslant \theta \leqslant 2\pi)$ and $x (-L \leqslant x \leqslant L, L \to \infty)$ is R_1, a constant which can be determined by prescribing the

volume flux of each fluid in the linear theory of stability. Denote the viscosity and the density for the fluid 1 and fluid 2 as (μ_1, ρ_1) and (μ_2, ρ_2), respectively. The radius of the pipe is R_2.

We scale the length with the mean radius of the core R_1, the velocity with the centre line velocity of the base flow W_0, pressure with $\rho_1 W_0^2$ and time with R_1/W_0. The base flow for these two fluids can be expressed as

$$U = (0, 0, W(r)) \quad \text{and} \quad \mathrm{d}P/\mathrm{d}x = -f, \tag{1}$$

where f is the constant pressure gradient acting along the pipe in the positive x-direction, and the axial velocity component is given by

$$W(r) = \begin{cases} 1 - mKr^2/A, & \text{in the core } 0 \leqslant r \leqslant 1 \\ [a^2 - r^2 - 2(K-1)\ln(r/a)]/A, & \text{in the annulus } 1 \leqslant r \leqslant a, \end{cases} \tag{2}$$

with

$$A = mK + a^2 - 1 + 2(K-1)\ln a, \tag{3}$$

$$a = \frac{R_2}{R_1}, \quad m = \frac{\mu_2}{\mu_1}, \quad \zeta = \frac{\rho_2}{\rho_1}, \quad K = \frac{f + \rho_1 g}{f + \rho_2 g}. \tag{4}$$

The centreline velocity of the base flow is given as

$$W_0 = \frac{f + \rho_2 g}{4\mu_2} R_1^2 A. \tag{5}$$

The parameter K relates the ratio of the pressure gradient to the force of gravity g. Alternatively, as in Chen *et al.* (1990), another parameter $\mathbb{R}_g$ could be introduced:

$$\mathbb{R}_g = g R_1^3 (\rho_1/\mu_1)^2. \tag{6}$$

$\mathbb{R}_g$ is negative in upward flow and positive in downward flow, and is zero for flows in horizontal pipes with the density of the two fluids matched. The parameters K and $\mathbb{R}_g$ are related through

$$K = \frac{4m\mathbb{R} - (\zeta - 1)\mathbb{R}_g(a^2 - 1 - 2\ln a)}{4m\mathbb{R} + (\zeta - 1)\mathbb{R}_g(m + 2\ln a)}, \tag{7}$$

where $\mathbb{R} = \rho_1 W_0 R_1/\mu_1$ is the Reynolds number. With this formulation, by choosing proper values of $\mathbb{R}_g$, we can study the instability of core–annular flows both in horizontal pipes and in vertical pipes either for upward flow or for downward flow. By adjusting the parameters we can also calculate the instability of thermal plumes in free rise or free fall ($f = 0$) due to buoyancy.

3. Disturbance equations and numerical solution

We perturb the core–annular flow by writing (u, v, w, p) for the perturbations in the velocities and pressure, and δ for the perturbation in the interface radius. We introduce the dimensionless surface tension parameter

$$J = TR_1\rho_1/\mu_1^2, \tag{8}$$

where T is the interfacial tension between two fluids. The linear stability for the vertical

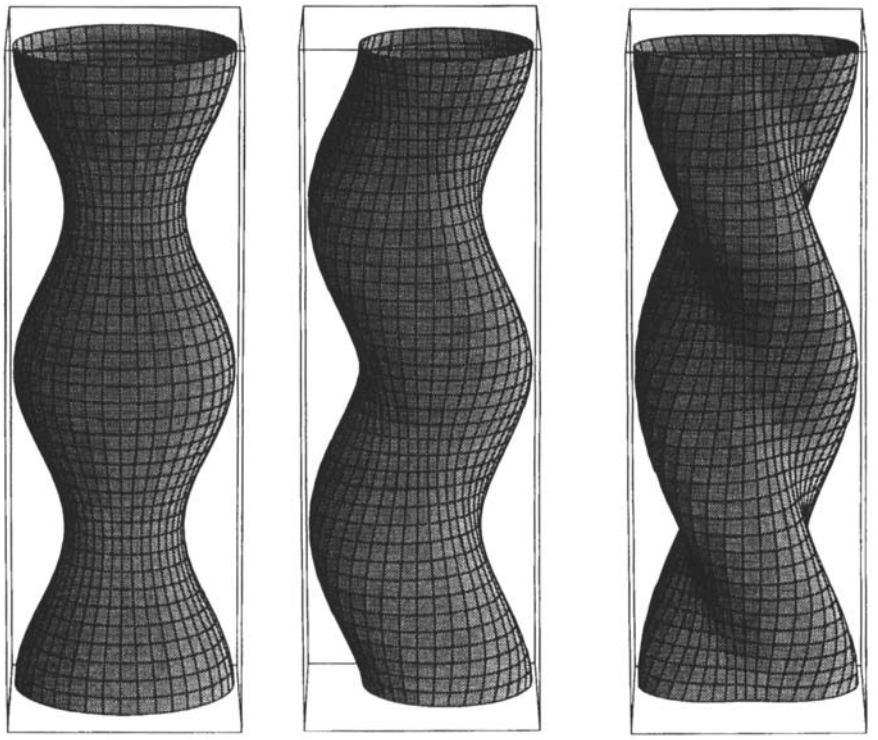

FIGURE 1. Geometric representations of various modes of interfacial waves.

core–annular flow can be analysed in the usual way by introducing the normal mode decomposition for disturbances

$$[u, v, w, p](r, \theta, x, t) = [iu, v, w, p](r) \exp[in\theta + i\alpha(x - ct)], \tag{9}$$

and

$$\delta(\theta, x, t) = \delta \exp[in\theta + i\alpha(x - ct)], \tag{10}$$

where $u(r), v(r), w(r), p(r)$ are complex-valued functions, and δ is a complex constant. The integer n is the wavenumber of disturbances in the azimuthal direction, and α is the wavenumber in the x-direction. c is generally complex: its real part represents the travelling wave speed of the disturbances, and its imaginary part measures the rate of growth or decay of the disturbances. The $n = 0$ mode represents the axisymmetric or varicose mode, and the $n = 1$ mode is the asymmetric (sinuous or snake) mode which resembles the corkscrew waves observed in experiments. Figure 1 shows the geometric representation of these modes. Certainly the interfacial waves shown are highly nonlinear, and the linear stability theory is only valid for infinitesimal disturbances. However, previous studies show that linear stability theory works amazingly well even in nonlinear regimes, see Joseph & Renardy (1992) and Miesen *et al.* (1992).

The linearized equations of motion are the same as (5.2)–(5.5) in Preziosi *et al.* (1989). The form of boundary and interfacial conditions are the same as their (5.6)–(5.11) with (5.9) replaced by (4.1) in Chen *et al.* (1990). In all the equations and the boundary and interfacial conditions the form of the base flow has to be replaced by (2).

These coupled linear ordinary equations constitute a general eigenvalue system for

c. The equations can be combined by eliminating w and p. Then they are solved using a Galerkin finite element method (Hu & Joseph 1989). We again take the cubic Hermite polynomials as the interpolation functions for u and the linear functions for v, since the governing equation for u after eliminating w is fourth order while the equation for v is second order. After discretization, we obtain a general complex-valued eigenvalue system

$$\boldsymbol{A}\boldsymbol{x} = c\boldsymbol{B}\boldsymbol{x}, \tag{11}$$

where $c = c_r + \mathrm{i}c_i$ is an eigenvalue introduced in (9) and (10), $\boldsymbol{A}$ and $\boldsymbol{B}$ are global matrices of $3N \times 3N$, $\boldsymbol{x} = [u_1, u_1', v_1, u_2, u_2', v_2, \ldots, u_N, u_N', v_N]^T$, N is the total number of nodes and $u' = \mathrm{d}u/\mathrm{d}r$. The eigen system (11) is solved with the routine DEIGZC in the library of IMSL10.

To resolve the boundary layers at the interface and at the pipe wall, non-uniform elements were introduced, see Hu *et al.* (1990). The size of the elements increases gradually as the distance from the interface or the pipe wall increases. The size of the smallest element is kept around $0.3(m/\mathbb{R}\alpha)^{1/2}$. Thus the number of elements used in the program varies automatically according to the values of m, $\mathbb{R}$ and α.

The eigenvalue c in (11) depends on all the parameters involved in the problem. They are listed as $(a, m, \zeta, J, \mathbb{R}_g, \mathbb{R}, n, \alpha)$. In this study we shall examine the growth (or decay) rate αc_i of various modes of disturbances as the other parameters vary. Generally, we plot the variation of the growth rate αc_i versus the wavenumber α, and compare the maximum growth rate reached by the $n = 0$, $n = 1$ and higher modes.

4. Results and discussion

First we check the stability profiles for flows under the experimental conditions documented in table 1 of Bai *et al.* (1992). The growth rates for various modes of disturbances are computed. For example, in their experiment number 6, the parameters for this downward flow are given as

$$(a, m, \zeta, J, \mathbb{R}_g, \mathbb{R}) = (1.7,\ 0.001\,66,\ 1.1,\ 0.06,\ 0.488,\ 1.2).$$

The inner diameter of the pipe in their experiment is 0.952 cm. Corkscrew waves were observed under these flow conditions. The measured wavelength and the wave speed are 3.3 cm and 43.12 cm s^{-1}, respectively, which were provided to us privately and were not reported in their original paper. The variation of the growth rate with the wavenumber of disturbances is shown in figure 2. The maximum growth rate for the asymmetric sinuous mode $n = 1$ is the largest. This mode is clearly the most dangerous one which would give rise to the corkscrew wave shown in figure 1. The wavelength corresponding to the maximum growth for this corkscrew wave is predicted as $L = 2\pi R_1/0.531 = 3.31$ cm, and the wave speed is calculated as $W_s = 1.422\,W_0 = 40.5$ cm s^{-1}. These values agree excellently with the experimental data. Growth rates for the higher modes ($n \geqslant 2$) are much smaller and negative, thus the higher modes of disturbances are stable.

Next we examine the effects of various parameters on the stability of the asymmetric sinuous mode of disturbances and identify the conditions where this mode is the most dangerous one.

Figure 3 presents the effects of the radius ratio of the pipe and the core, a, keeping the other parameters fixed. As a reduces to one, the core gets thicker. At small a, owing to the confinement of the pipe wall, the axisymmetric mode $n = 0$ is always the most unstable one as shown in figure 3(c), although the maximum growth rates for the

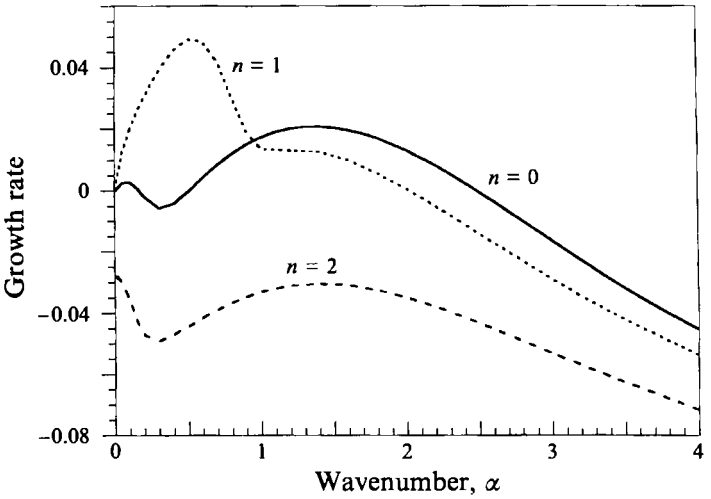

FIGURE 2. Growth rates versus wavenumber for axisymmetric and asymmetric disturbances. The flow conditions are taken the same as the experiment No. 6 in Bai *et al.* (1992).

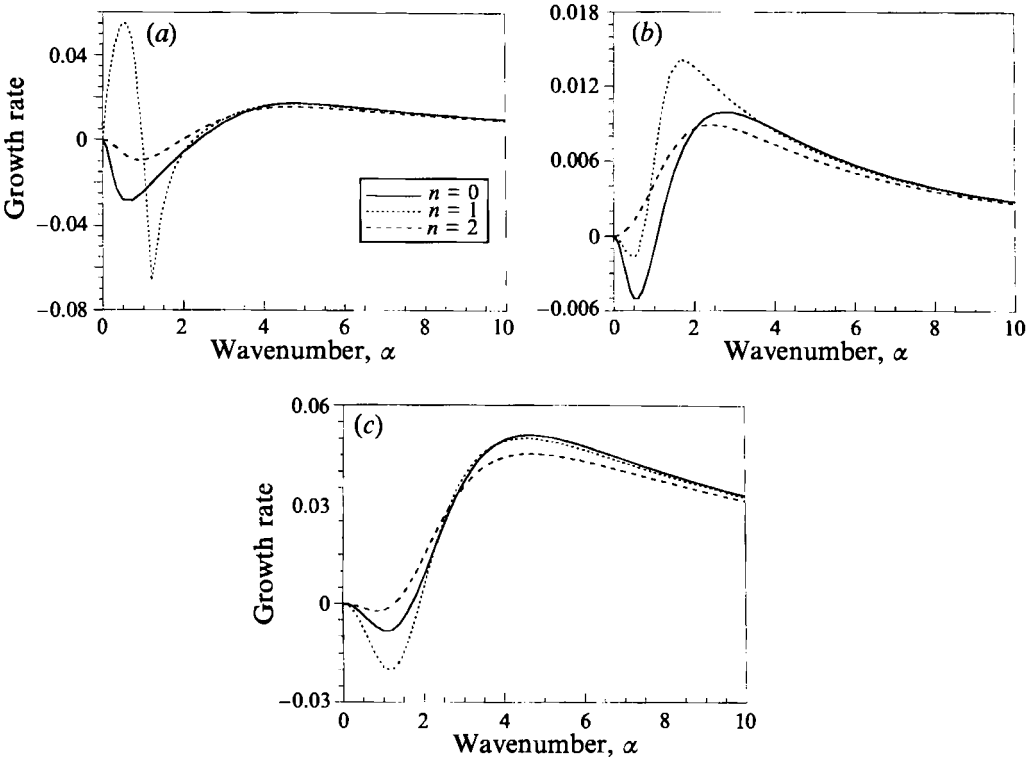

FIGURE 3. Effects of the radius ratio of the pipe to the core a, for $m = 0.1$, $\zeta = 1.1$, $J = 0$, $R_g = 1$, $R = 1$. (*a*) $a = 2$, (*b*) $a = 1.4$, (*c*) $a = 1.2$.

$n = 0$ and $n = 1$ modes may be very close. Figures 3(*a*) and 3(*b*) indicate that the asymmetric sinuous mode $n = 1$ is the most unstable mode when the core is thin, and there is a critical radius of the core below which this asymmetric mode overtakes the axisymmetric mode to become the most unstable disturbance. For the specific case

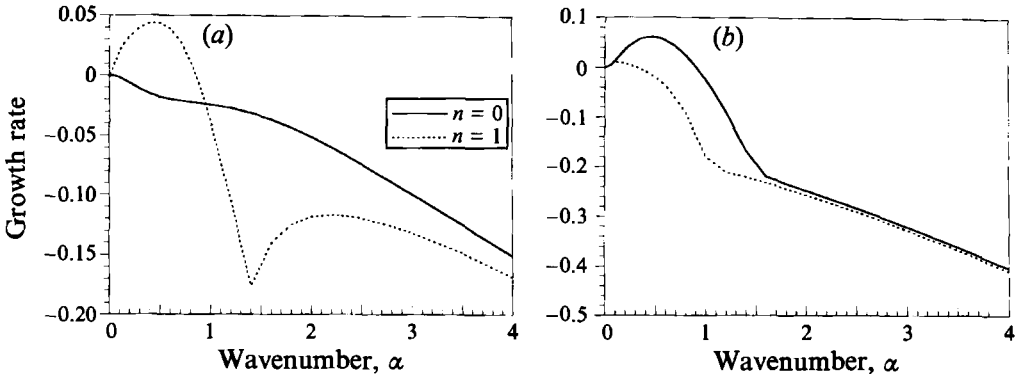

FIGURE 4. Effects of the interfacial tension parameter J: (*a*) $J = 0.1$, (*b*) $J = 1$; other parameters as figure 3(*a*).

indicated in figure 3, the critical radius is slightly smaller than 1.4. When the sinuous mode becomes the dominant unstable mode, the critical wavenumber where the growth rate reaches maximum is relatively small, $\alpha_c \approx 0.54$ or the wavelength $L = 2\pi R_1/\alpha_c \approx 11.6R_1$ as shown in figure 3(*a*). The relatively long wavelength of corkscrew wave agrees with general experimental observations. The growth rate for the $n = 1$ mode in figure 3(*a*) shows two peaks: a sharp peak at small wavenumber and a flat one at large wavenumber. These two peaks correspond to two different modes of instability. The sharp peak is related to the corkscrew waves and is a distinctive feature for the asymmetric sinuous mode, while the flat peak is shared by all modes of disturbances. As the core gets thicker ($a \to 1$), the asymmetric sinuous mode shifts to larger wavenumbers, and its growth rate reduces and is eventually overtaken by the flat peak.

The effects of the interfacial tension on the growth rates of different modes of disturbances are shown in figure 4. Here, only the $n = 0$ and $n = 1$ modes are considered. The parameters involved are kept the same as in figure 3(*a*) except that the surface tension parameter J is increased from 0 to 0.1 and 1. Comparing figures 3(*a*), 4(*a*) and 4(*b*), it is quite clear that the interfacial tension stabilizes the short waves (disturbances with large wavenumbers). As J increases, the dominance of the $n = 1$ mode disappears, since at large J the capillary instability is the main mechanism of instability where the axisymmetric mode is the most unstable one. For long waves, as in the case of corkscrew waves, the interfacial tension should have a relatively small effect.

We next examine the effects of the Reynolds number of the flow. The growth rates for the $n = 0$ and the $n = 1$ modes are presented in figure 5. Again, the parameters are kept the same as in figure 3(*a*) except that the Reynolds number $\mathbb{R}$ is increased from 1 to 10 and 100. As the Reynolds number increases, the shear at the surface of the core increases. Figures 3(*a*), 5(*a*) and 5(*b*) clearly show that this shear has a stabilizing effect on the asymmetric mode of disturbance, similar to the case when the radius of the core is close to the radius of the pipe. At large $\mathbb{R}$, the instability is related to the emulsification of oil in water as indicated in Hu & Joseph (1989). For this mode of instability, the maximum growth rate for the axisymmetric mode is larger than that of the non-axisymmetric modes, although they are very close. This behaviour of the growth rates for various modes agrees with the result of Boomkamp & Miesen (1992) in the limit of the small parameter $\epsilon = m/\mathbb{R}\alpha$. It is shown by Preziosi *et al.* (1989) that

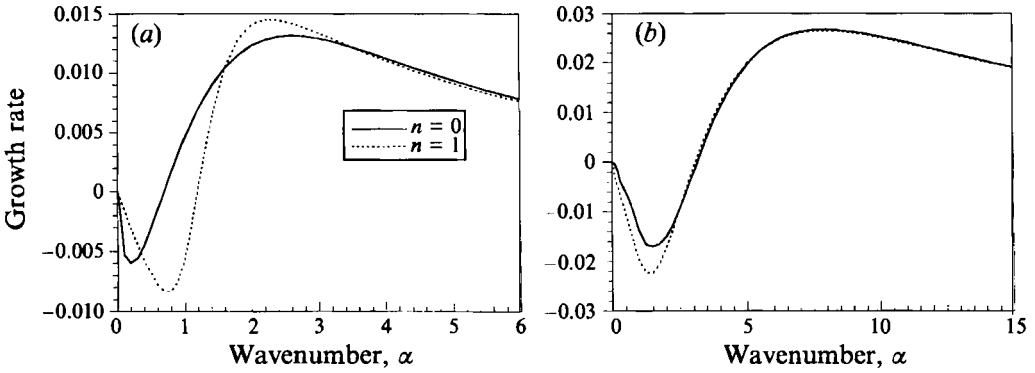

FIGURE 5. Effects of the Reynolds number R of the flow: (*a*) $R = 10$, (*b*) $R = 100$; other parameters as figure 3(*a*).

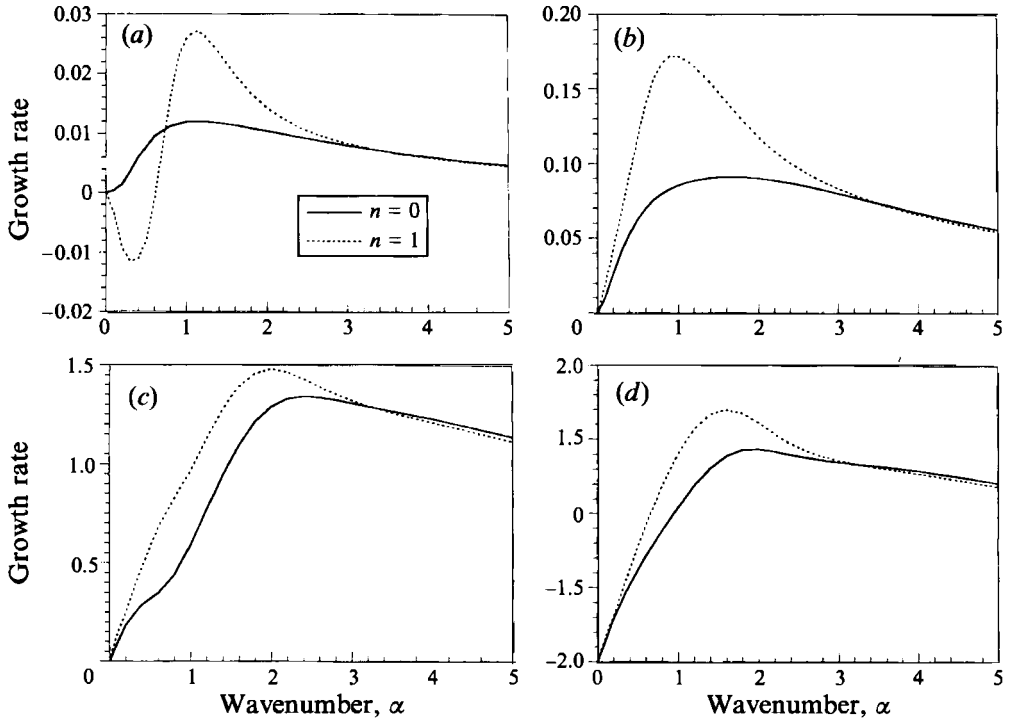

FIGURE 6. Effects of the gravity R_g: (*a*) $R_g = 0$, (*b*) $R_g = -1$, (*c*) $R_g = 10$, (*d*) $R_g = -10$; other parameters as figure 3(*a*).

the growth rate for various modes of disturbances tends to zero for very long waves $\alpha \to 0$. However, in this long-wave limit the parameter ϵ is no longer small, and the analysis of Boomkamp & Miesen is not valid, which is clearly indicated in their figure 2. We computed growth rates for various modes of disturbances under the same conditions as in their figure 2 in order to estimate the range of validity of their perturbation analysis. We found excellent agreement between our numerical result and their analytic one for wavenumbers $\alpha \geqslant 30$ (or $\epsilon \leqslant 3.3 \times 10^{-7}$). Their result fails at

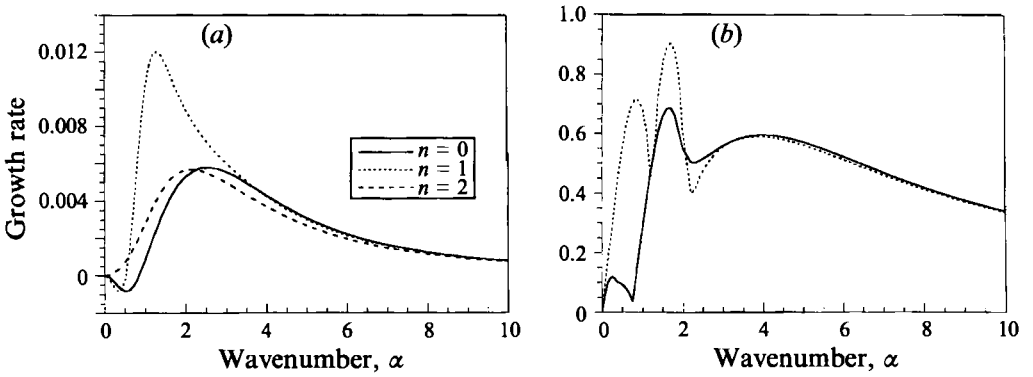

FIGURE 7. Effects of the viscosity ratio m: (*a*) $M = 0.1$, (*b*) $m = 0.001$; other parameters as figure 3(*a*).

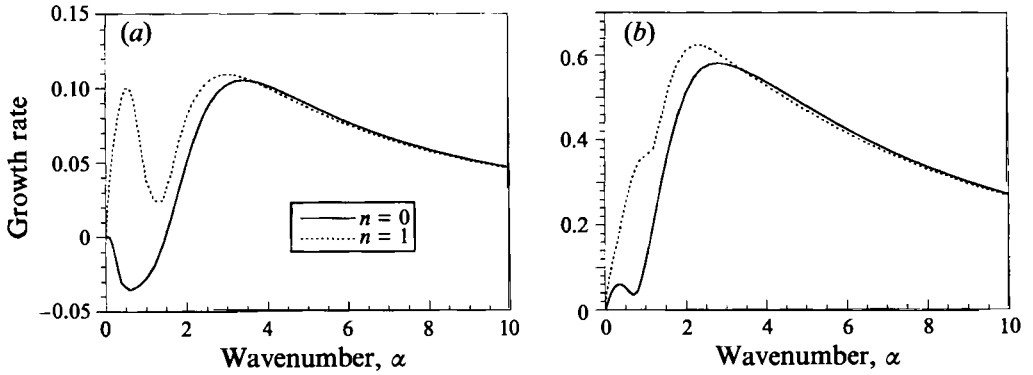

FIGURE 8. Effects of the density ratio ζ: (*a*) $\zeta = 1.2$, (*b*) $\zeta = 1.5$; other parameters as figure 3(*a*).

wavenumbers $\alpha \leqslant 4$ (or $\epsilon \geqslant 2.5 \times 10^{-6}$), which is very restrictive. Our results presented in this study are obtained outside the validity of their analysis, thus the dominance of the asymmetric sinuous mode reported here is of a different nature.

Under the conditions where the asymmetric sinuous mode is the most dangerous mode, as indicated in figure 3(*a*), we now examine the effects of the gravity. Figure 6 shows the variation of the growth rate at different values of R_g. We note that in a vertical pipe, R_g is positive for downward flow and negative for upward flow, and in a horizontal pipe with the gravity neglected, R_g is zero. Figure 6(*a*) demonstrates that even in a horizontal pipe, the asymmetric sinuous mode is the most dangerous one, when the flow condition is right. The same asymmetric mode of disturbance also dominates the upward flow as shown in figure 6(*b*). This asymmetric mode of instability persists both in the upward and downward flows as the gravity parameter R_g is increased, shown in figures 6(*c*) and 6(*d*) for $R_g = 10$ and -10.

The next important factor in the instability of the asymmetric sinuous mode of disturbance is the viscosity ratio m. Figures 7(*a*), 3(*a*) and 7(*b*) depict the variation of the growth rates as the viscosity ratio m is changed from 0.1 to 0.01 and 0.001. For these three cases, $n = 1$ is the most dangerous mode. However, as m decreases, there are various peaks in the growth rate, indicating the existence of different modes of instability at different regimes of wavenumber α.

Figure 8 presents the effects of a density difference between the two fluids. Figures

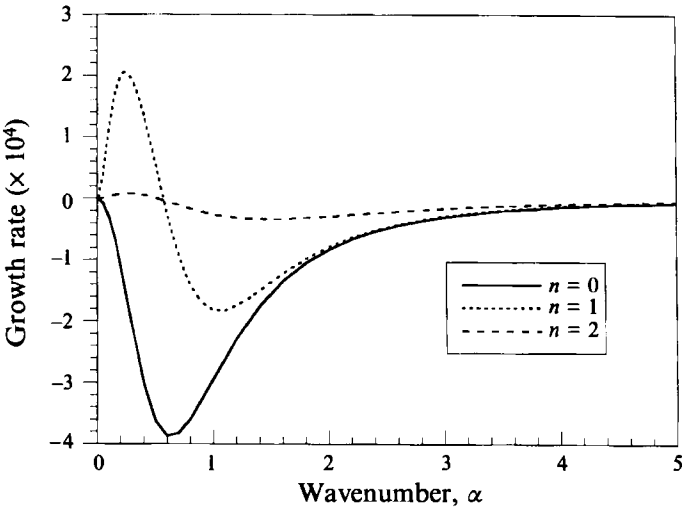

FIGURE 9. Free rise of a thermal plume: $a = 5$, $m = 1$, $\zeta = 1.1$, $J = 0$, $\mathcal{R}_g = 1$, $\mathcal{R} = 6.77$.

8(a) and 8(b) demonstrate that the $n = 1$ mode is still the most unstable mode as the density ratio ζ of the two fluids is increased from 1.1 to 1.2 and 1.5.

Yang (1992) showed a picture of the non-axisymmetric transition of rising cigarette smoke in his figure 1b. The diameter of the smoke column is about 0.1 cm, and the wavelength of the sinuous wave on the column is about 1.4 cm (measured directly from the picture) when the smoke column just becomes unstable. Thus the ratio of the wavelength to the diameter of the smoke column is around 14.

In our theory, the stability of a freely rising thermal plume (or smoke column) in ambient air was calculated by using a large radius ratio ($a = 5$) and matching the viscosities of the two fluids ($m = 1$). The plume rises due to the density difference between the hot (plume, core) and cold (surrounding) air. No pressure gradient is imposed. In this situation the Reynolds number of the flow $\mathcal{R}$ is related to the parameter $\mathcal{R}_g$ through the relation (7) where K is given by (4) with the pressure gradient $f = 0$. Figure 9 indicates that for this freely rising plume the asymmetric mode is the only unstable mode. The wavenumber where the growth rate reaches maximum is $\alpha_c = 0.24$ which corresponds to a wavelength about 13.1 times the diameter of the rising plume. This wavelength agrees with experimental observation of Yang (1992). The agreement is quite robust, since for density ratios less than 1.5 the predicted wavelength does not change. The density ratio ζ is determined by the temperature difference between the hot and cold air, and $\zeta = 1.5$ corresponds to the condition that the temperature of the plume is about 300 °C above the ambient temperature.

In the analysis of Yang (1992), the two fluids are assumed inviscid and the plume is found to be unstable to short waves (Hardmard instability). This study goes beyond the analysis of Yang in that it includes all physical factors which influence the stability of the plume and predicts a unique wavelength for the instability.

The mechanisms of the instabilities can be elucidated by examining the terms involved in the equation governing the evolution of the energy of a small disturbance, as introduced by Hu & Joseph (1989). This energy balance may be evaluated at the most unstable mode of the disturbance. Bai *et al.* (1992) identified that the bamboo waves ($n = 0$ mode) were driven by interfacial friction. In this study, we performed the same energy-budget calculation, and found that the interfacial friction is also the

driving mechanism for the corkscrew waves ($n = 1$ mode). This instability may be visualized as the buckling of the core under the action of the shear stress at the surface of the core as suggested by Bai *et al.* (1992).

5. Conclusions

This study of the stability of core–annular flow of water and oil with respect to non-axisymmetric disturbances gives rise to the following conclusions:

(i) When the oil core is thin, the flow is most unstable to the asymmetric sinuous mode of disturbances, and the core moves in a form of corkscrew waves as observed in experiments. However, as the radius of the core approaches the radius of the pipe, the axisymmetric mode of disturbance becomes the most unstable one. The pipe wall has a confining effect on the asymmetric disturbances.

(ii) The asymmetric mode of disturbance is the most dangerous mode for a relatively wide range of parameters, except in the cases when the effect of interfacial tension is large, where the capillary instability dominates, and when the Reynolds number is large, where the emulsion of water in oil occurs. When the flow conditions are right, the asymmetric mode of instability persists in vertical pipes with upward and downward flows and in horizontal pipes.

(iii) The application of this analysis to the study of the instability of a freely rising thermal plume indicates that the asymmetric mode of disturbance is the most unstable mode. The analysis also predicts a unique wavelength of the asymmetric sinuous mode of disturbance, which agrees with experimental observations.

This work is supported by the Laboratory for Research on the Structure of Matter at the University of Pennsylvania through NSF Grant DMR91-20668 and by a grant from the Research Foundation of University of Pennsylvania. We thank Mr R. Bai for providing us with his original experimental data.

REFERENCES

BAI, R., CHEN, K. & JOSEPH, D. D. 1992 Lubricated pipelining: stability of core–annular flow Part 5. Experiments and comparison with theory. *J. Fluid Mech.* **240**, 97–132.

BOOMKAMP, P. A. M. & MIESEN, R. H. M. 1992 Nonaxisymmetric waves in core–annular flow with a small viscosity ratio. *Phys. Fluids* A **4**, 1627–1636.

CHEN, K., BAI, R. & JOSEPH, D. D. 1990 Lubricated pipelining. Part 3. Stability of core–annular flow in vertical pipes. *J. Fluid Mech.* **214**, 251–286.

FREEMAN, R. W. & TAVLARIDES, L. L. 1979 Observation of the instabilities of a round jet and the effect of concurrent flow. *Phys. Fluids* **22**, 782–783.

HICKOX, C. E. 1971 Instability due to viscosity and density stratification in axisymmetric pipe flow. *Phys. Fluids* **14**, 251–262.

HU, H. H. & JOSEPH, D. D. 1989 Lubricated pipelining: stability of core–annular flow. Part 2. *J. Fluid Mech.* **205**, 359–396.

HU, H. H., LUNDGREN, T. S. & JOSEPH, D. D. 1990 Stability of core-annular flow with very small viscosity ratio. *Phys. Fluids* A **2**, 1945–1954.

JOSEPH, D. D. 1990 Separation in flowing fluids. *Nature* **348**, 487.

JOSEPH, D. D. & RENARDY, Y. 1992 *Two-Fluid Dynamics*. Springer.

JOSEPH, D. D., RENARDY, Y. & RENARDY, M. 1984 Instability of the flow of immiscible liquids with different viscosities in a pipe. *J. Fluid Mech.* **141**, 309–317.

LISTER, J. R. 1987 Long-wavelength instability of a line plume. *J. Fluid Mech.* **175**, 413–428.

MIESEN, R., BEIJNON, G., DUIJVESTIJN, P. E. M., OLIEMANS, R. V. A. & VERHEGGEN, T. 1992 Interfacial waves in core–annular flow. *J. Fluid Mech.* **238**, 97–117.

PREZIOSI, L., CHEN, K. & JOSEPH, D. D. 1989 Lubricated pipelining: stability of core–annular flow. *J. Fluid Mech.* **201**, 323–356.

RENARDY, Y. 1987 Viscosity and density stratification in vertical Poiseuille flow. *Phys. Fluids* **30**, 1638–1648.

YANG, H. Q. 1992 Buckling of a thermal plume. *Intl J. Heat Mass Transfer* **35**, 1527–1532.